J. Phys.: Condens. Matter 1 (1989) 7367–7384. Printed in the UK

A comparison of defect energies in MgO using Mott–Littleton and quantum mechanical procedures

R W Grimes†, C R A Catlow† and A M Stoneham‡
Theoretical Physics Division, Harwell Laboratory, Didcot, Oxon OX11 0RA, UK

Received 10 April 1989

Abstract. We compare the predictions of Mott–Littleton calculations, based on empirical interatomic potentials, with predictions based on self-consistent solutions of the Schrödinger equation for embedded clusters. Simple vacancy and substitutional defects in MgO are modelled using both the classical Mott–Littleton and quantum mechanical methods. Particular attention is paid to the size of the quantum mechanical cluster, the different ways that polarisation is taken into account and the choice of basis set. Results are presented for closed-shell systems only, namely V''_{Mg} and $V^{\cdot\cdot}_{O}$ vacancies and for Li'_{Mg}, Na'_{Mg}, $Al^{\cdot}_{Mg}$, $F^{\cdot}_{O}$ and $Cl^{\cdot}_{O}$ substitutional impurities. We find a respectable level of agreement between the quite distinct approaches. This both validates the classical calculations and indicates useful generalisations combining the two approaches.

1. Introduction

There has been considerable success in modelling closed-shell defects in ionic crystals using techniques based on the Mott–Littleton method employing shell-model interatomic potentials [1]. Yet, in such modelling, it is often necessary to make approximations for centres in which solution of the Schrödinger equation would be desirable. In principle, a general approach is possible, combining a quantum treatment of an inner region with a shell-model description of its environment, as in the recent studies of Vail and co-workers [2, 3] and Harding and co-workers [4]. This is still a costly approach, however, and in the present paper we explore similar methods in which quantum cluster calculations are embedded in an array of point charges. Our aim is, by comparing different methods, to elucidate those features that are necessary for reliable cluster calculations on closed-shell defects. Conversely, we are able to show how Mott–Littleton calculations on defects in oxides can be underwritten by more rigorous quantum mechanical methods.

Our study concentrates on MgO, and the defect centres chosen are all closed-shell systems, namely the simple vacancies $V^{\cdot\cdot}_{O}$, and V''_{Mg}, and the substitutional ions Li'_{Mg}, Na'_{Mg}, $Al^{\cdot}_{Mg}$, $F^{\cdot}_{O}$ and $Cl^{\cdot}_{O}$. Because MgO has the rock-salt structure, all the defect sites have octahedral symmetry (see figure 1) which is retained in the present work (thus we ignore the off-centring of the Li'_{Mg} substitutional ion). These simple defect centres

† Also at Department of Chemistry, University of Keele, Keele, Staffs ST5 5BG, UK.
‡ Present address: Materials Physics and Metallurgy Division, Harwell Laboratory, Didcot, Oxon OX11 0RA, UK.

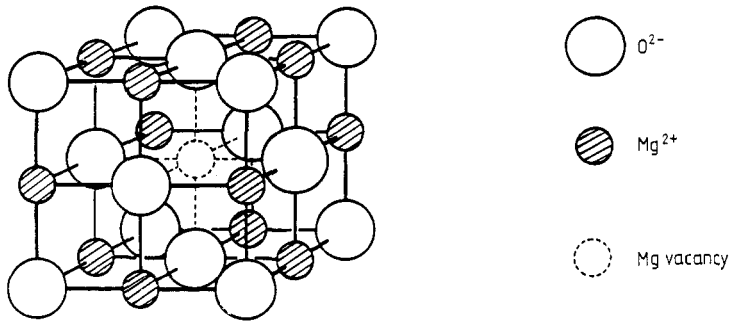

Figure 1. Example of the type of point defect in MgO to be modelled.

are both interesting in themselves and an essential starting point for the study of more complex defect processes in oxides [5–7] and they have been extensively studied by Mott–Littleton methods. The present study is the first detailed investigation using quantum mechanical calculations (although calculations of other defects, e.g. the F^+ centre [2, 3] have been reported in recent years).

2. Theoretical method

In this section we review the essential features of the Mott–Littleton and quantum mechanical cluster methods employed in these studies.

2.1. Mott–Littleton methods

The classical Mott–Littleton method with Newton–Raphson minimisation (coded in the HADES [8] and CASCADE [9] codes) is essentially a simple technique. The crystal is partitioned into two regions. Region I is treated explicitly, and ions are relaxed to zero force. The surrounding region II is treated more approximately by calculating the polarisation due to the effective charge of the defect. An interface region IIa is included in which displacements are calculated using the simple Mott–Littleton procedure, but in which interactions with region I are calculated by explicit summation.

In region I, short-range potentials must be specified between ions. In the present study we used the MgO potential parameters reported in the appendix. Note that the short-range potentials on ions are parametrised in such a way as to include dispersion terms and that special care was needed in deriving impurity–lattice potentials as described in the appendix. In Mott–Littleton calculations electronic polarisation effects are treated using the shell model [10]. In the present study, we shall assume only oxygen ions are polarisable; this, we shall see, causes only small errors.

We shall introduce two further simplifications to make the comparison between Mott–Littleton and cluster approaches easier. First, whilst it is normal to define short-range potentials between all ions in regions I and IIa, we shall only include those short-range interactions that are also modelled in the quantum mechanical model. Second, the ions of region IIa will be frozen in the present calculations. In this manner it will be possible to compare directly the effect of the empirical short-range potentials with interactions calculated quantum mechanically *in situ*. All the Mott–Littleton calculations in this study use the CASCADE code [9].

Table 1. Details of point-ion cluster in GAMESS.

		Electrostatic field (eV Å^{-1})		
Ion[a]	Madelung potential (eV)[b]	E_x	E_y	E_z
000	−47.7938	0.0000	0.0000	0.0000
100	−47.7955	−0.0530	0.0000	0.0000
Ion	Charge[c]	Number of ions		
100	−2.00	6		
110	+2.00	12		
111	−2.00	8		
200	+2.00	6		
210	−2.00	24		
211	+1.602564	24		
300	+0.268164	6		

[a] We designate the position of an ion relative to the central defect site as A B C where the integers A, B and C represent the number of magnesium–oxygen distances (2.106 Å) away from the central defect in cartesian coordinates along the main crystal axis.
[b] The Madelung potential at both oxygen and magnesium bulk crystal sites was calculated from CASCADE as being −47.7933 eV and the fields at both sites are zero.
[c] This case is for a magnesium-centred defect cluster.

2.2. *Quantum cluster methods*

Our approach here again employs two regions. In this case, calculations in the inner region use an *ab initio* Hartree–Fock, self-consistent-field (SCF) molecular-orbital approach. This technique, even when used in its single-determinantal form, is still costly in terms of computer time. Consequently, region I can include only the defect centre and a small number of lattice ions, perhaps one or two shells. This is much smaller than the practical limit upon region I of the Mott–Littleton method which may include hundreds of ions. An SCF wavefunction with a suitable basis set will include some representation of electronic polarisation, although the single-determinantal calculation will not model any correlation contributions.

The outer region in our present quantum mechanical calculations consists of roughly 100 point charges positioned at lattice sites in consecutive complete shells surrounding the inner region cluster. Each ion is modelled as a fixed point charge. The positions of these point charges are not adjusted during the calculation unlike the more sophisticated procedure employed by Vail and co-workers [2–4]. These point charges model the dominant long-range Coulombic interactions; beyond the inner region, the short-range repulsive potentials have essentially relatively little effect on the defect centre. The ions in the outermost shell of the outer region have non-integral charges, the values being chosen to give the correct infinite-crystal Madelung potentials and electrostatic fields in the inner region, that is, on the ions within the quantum mechanical cluster. All other ions in the outer region assume their formal charge states. Full details of the point charge cluster are given in table 1. It is important to realise that the outer region ions do not respond at all to the introduction of a defect centre in the inner region so the outer region is treated quite differently from that in CASCADE, and is not equivalent to region II in the Mott–Littleton method. All quantum mechanical calculations reported in this study use the GAMESS code [11].

3. Definitions of energies

In order to facilitate the comparison of Mott–Littleton and quantum cluster calculations, it is necessary to define carefully the terms that are used.

3.1. Defect formation energies

The results of calculations will be discussed using the following equation for the defect formation energy:

$$\begin{matrix}\text{Total energy to}\\ \text{form defect}\end{matrix} = \begin{matrix}\text{Energy to create}\\ \text{unrelaxed defect}\end{matrix} + \begin{matrix}\text{Relaxation}\\ \text{energy.}\end{matrix}$$

Thus, we first calculate the energy to form the defect in the perfect lattice, with all nuclear positions unrelaxed. Relaxation of nuclear positions or (in the case of Mott–Littleton calculations) nuclear and shell positions is then allowed. The difference in energy between the relaxed and unrelaxed lattice is the relaxation energy.

Consider the creation of an unrelaxed defect centre. The ion occupying the lattice site which is to become the defect centre is removed to infinity. The energy required to form a vacancy defect is therefore given by:

$$\begin{matrix}\text{Unrelaxed vacancy}\\ \text{formation energy}\end{matrix} = \begin{matrix}\text{Energy of}\\ \text{defective}\\ \text{lattice}\end{matrix} - \begin{matrix}\text{Energy of}\\ \text{perfect}\\ \text{lattice}\end{matrix} + \begin{matrix}\text{Self-energy}\\ \text{of displaced}\\ \text{ion.}\end{matrix}$$

In the case of the quantum mechanical cluster calculation, the energy of the perfect lattice refers to the total energy of the quantum mechanical cluster and to its surrounding point charge array before the defect has been created. If a substitutional ion is to be incorporated at the vacancy site, it is assumed to be brought from infinity so that the formation of an unrelaxed substitutional ion defect also includes the self-energy of the substitutional ion, since:

$$\begin{matrix}\text{Unrelaxed}\\ \text{substitutional}\\ \text{formation energy}\end{matrix} = \begin{matrix}\text{Energy of lattice}\\ \text{incorporating the}\\ \text{substitutional ion}\end{matrix} - \begin{matrix}\text{Energy of}\\ \text{perfect}\\ \text{lattice}\end{matrix} + \begin{matrix}\text{Self-energy}\\ \text{of displaced}\\ \text{ion}\end{matrix}$$

$$- \begin{matrix}\text{Self-energy}\\ \text{of substitutional}\\ \text{ion.}\end{matrix}$$

3.2. Self-energies of ions

In the Mott–Littleton calculation, the self-energy of an ion is zero because the potentials are defined to be zero at infinite interatomic separation. In the quantum cluster calculations however, the isolated ion does have an electronic structure and hence the self-energy must be calculated explicitly. This is achieved by performing the same calculation on the ion embedded in a point-charge cluster, except that point charges are now used to represent all the ions surrounding the central ion. The pure Madelung term in the calculated total energy has been subtracted out. This correction may not be perfect, as the wavefunction of the ion in the point-charge cluster will differ somewhat from that in an appropriate quantum mechanically treated cluster, since the adjacent ions that generally act on the central ions's electrons, and help to confine them to the atomic

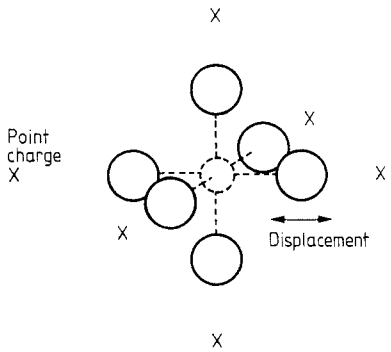

Figure 2. Example of the size of quantum mechanical cluster used in an unrelaxed defect calculation.

centre, are missing as the central ion is simply surrounded by point charges. Consequently, the electrons tend to spill out a little onto the surrounding point charges. However, this effect leads to energy terms that are very small compared with the total defect energy. In future, we plan to investigate this correction term by using pseudopotentials on the nearest-neighbour ions in the self-energy calculation in order to contain the charge density.

4. Quantum cluster calculations: detailed methodology

This section will explore various methodological aspects of the cluster calculations, in particular the choice of basis sets and basis set superposition error.

4.1. Cluster size and choice of basis

The quantum cluster calculations on unrelaxed defects were carried out with quantum mechanical clusters of either MgO_6 for the magnesium-centred defect sites or Mg_6O for the oxygen-centred site (see figure 2). Such a small cluster size enabled the calculations to be repeated with a variety of basis sets. Three types of basis set were used. First, the simplest orbital representation STO 3G basis in which each Slater type orbital is modelled by a fixed sum of three Gaussian functions. Second, we use the SV 3-21G basis (split valence 3-21) where all the valence atomic orbitals are split from a sum of three Gaussians into two separate functions, with two Gaussians in one function and a single Gaussian in the other. The splitting increases the flexibility of the representation. Last, the most sophisticated basis is a triple zeta valence basis (TZV). In this, the lowest core orbitals are modelled by a sum of usually six Gaussians in order that they have a good functional shape. The valence orbitals are a set of independent Gaussians which gives the required flexibility.

4.2. Unrelaxed vacancy energies

The results for the formation energy of an unrelaxed oxygen vacancy ($V_O^{\cdot\cdot}$) calculated using the quantum cluster technique, for different basis sets, are compared with the values calculated using Mott–Littleton methodology in table 2. The important point to

Table 2. Formation energy of unrelaxed oxygen vacancy ($V_O^{\cdot\cdot}$): basis-set dependence in GAMESS calculations[a].

Basis[b] for oxygen ion	Basis for magnesium ion	Energy (eV)
TZV	TZV	42.064
TZV	SV3-21G	42.309
SV6-21G	SV6-21C	50.472
SV3-21G	SV3-21G	50.607
STO 3G	STO 3G	65.980

[a] For reference, the Mott–Littleton calculation gives a formation energy of 41.118 eV.
[b] Abbreviations are explained in the text.

Table 3. Total energies calculated from GAMESS (au) and their dependence on basis for a range of anions.

		Quantum mechanically modelled cluster size		
		Anion and (100) Mg ions	Anion only	Defect formation energy (au)
F^-	TZV	1342.8957	156.7986	0.7424
	SV3-21G	1342.3601	156.1316	0.6109
	Difference	0.5356	0.6670	
Cl^-	TZV	1703.1695	516.8601	0.5299
	SV3-21G	1700.9893	514.6772	0.5273
	Difference	2.1801	2.1829	
O^{2-}	TZV	1318.5328	132.5717	0.00[a]
	SV3-21C	1318.1260	131.8600	0.00
	Difference	0.4068	0.7117	

[a] As O^{2-} is the lattice ion, it has no associated 'defect' formation energy.

notice in these results is that as the quality of the basis improved from STO 3G to TZV, the defect formation energy from the quantum cluster calculation decreases and approaches the value calculated with Mott–Littleton methodology. Thus, a basis set for oxygen of the quality of TZV is needed in order to calculate reliable formation energies, whilst only SV 3-21G is required on magnesium ions. However, once this basis quality is achieved, the results of the two methods agree well. In general, we found that anions require a TZV basis but cations need only SV 3-21G. This is due to the more diffuse nature of the anion electron density and their high polarisability.

4.3. Substitutional defects

The use of a defect formation energy to indicate the quality of basis required to calculate reliable energies, as in table 2, can sometimes be misleading. Consider in table 3 the examples of the formation energy of $F_O^{\cdot}$ and $Cl_O^{\cdot}$. Both TZV and SV 3-21G bases are used for fluorine and chlorine but for magnesium only the SV 3-1G basis is employed. It is apparent that the basis sets give rise to very similar formation energies for $Cl_O^{\cdot}$ but rather

different values for $F_O^{\bullet}$. We might be tempted to conclude that, although the higher-quality TZV basis is required in fluorine, SV 3-21G suffices for chlorine. The result does indeed indicate that a TZV basis is needed on fluorine, but the converse result for chlorine is invalid. This can be seen by looking at the total energies for the individual chlorine defect clusters ($ClMg_6$ and Cl in point-charge arrays). We see a large decrease in total energy as the basis is improved, which shows that the better-quality basis still has a significant effect on the stability of the system. However, the decrease is equally large for both chlorine clusters, and the basis set effect cancels out in the final formation energy. In other words, the invariance of the defect formation energy with increasing basis set quality is a necessary but not sufficient condition that the lower-quality basis can be employed.

Table 3 also shows that the formation energy for $F_O^{\bullet}$ increases whereas that for $V_O^{\cdot\cdot}$ decreases as the basis is improved. For the various clusters, total energies may change with basis set by significantly different amounts, so that their differences may lead to increasing or decreasing formation energies, depending on the defect under investigation. On the other hand, the total energy of a particular cluster (e.g. $ClMg_6$ in a point-charge array) will always decrease with increasing basis set quality, consistent with the variational principle (see table 3).

4.4. Basis set superposition error (BSSE)

In table 2 we saw that as the quality of the oxygen basis was improved, the total cluster energies decreased. However, although TZV is indeed a relatively sophisticated basis set, the cluster energies (E_A) will still not have reached their Hartree–Fock limits. Therefore if a new set of orbitals is added to the cluster calculation, the cluster energy can be lowered still further towards the Hartree–Fock limit. This effect can lead to an error if we wish to calculate the energy associated with the addition of an extra atom to a cluster when using the simple sums of cluster energies as outlined in § 3.1. The addition of the new atom to a cluster provides orbitals that can be used by the existing cluster to lower its own energy towards the Hartree–Fock limit. The cluster ions will also provide orbitals that lower the Hartree–Fock energy of the new ion. This effect is in addition to the ordinary interaction energy (ΔE_{AB}). Thus, if E_B is defined to be the energy of the additional ion, and E_{AB} the energy of the new larger cluster, we have:

$$E_{AB} - E_A - E_B = \Delta E_{AB} + \Delta E_A + \Delta E_B$$

where ΔE_A and ΔE_B are the errors associated with the availability of new orbitals. These are known as the basis set superposition errors.

The values of ΔE_A and ΔE_B can be estimated by calculating total cluster energies in which the basis orbitals of the additional atom are included but in which its nucleus and electrons are left out. The difference between cluster energies with and without the extra basis gives the basis set superposition errors, and these can be included in the original sum. This form of error correction is called the 'function counterpoise method' (CP) [12].

It has been suggested [13] that this method of correcting for the BSSE provides an overestimate of the correction energy (for a discussion see reference [14]). The main criticism is that some of the orbitals made available in the correction calculation will be fully occupied in the complete cluster. Therefore, as the Pauli principle will prevent the full use of the core orbitals from the additional atom in the total cluster calculation, they should not be available in the correction calculation [13]. To allow for this, the 'virtual-only CP method' [15] can be used. Here only the virtual orbitals of the additional ion's

Table 4. Comparison of correction energies using the virtual-only and full functional counterpoise methods (all energies in eV).

Cluster		Virtual-only	Full
Isolated O (000)	– Isolated O (000) with additional basis from six virtual Mg at (100) sites	1.545	33.552
Isolated Mg (000)	– Isolated Mg (000) with additional basis from six virtual O at (100) sites	0.481	0.483
O_6 cluster with Mg vacancy (000)	– O_6 cluster with additional basis from a virtual Mg (000)	1.040	18.653
Mg_6 cluster with O vacancy (000)	– Mg_6 cluster with additional basis from a virtual O (000)	0.205	0.208

basis are considered in the BSSE correction calculations. We have considered both the virtual-only and full CP methods in calculating the values of ΔE_A and ΔE_B and, for reasons outlined below, have chosen to use the virtual-only method in the present work.

In table 4, we compare calculated values for ΔE_A and ΔE_B for the four different clusters types. The first two clusters involve a single cation or anion surrounded by the appropriate point-charge clusters. These were studied to examine the effect on the total cluster energy of the basis of the six nearest-neighbour (100) ions. The second two clusters, the anion and cation vacancy clusters O_6 and Mg_6 and their point charge arrays, were studied to determine the effect of the basis from the displaced (000) central ions.

Consider first the effect of an additional basis at the central vacancy site (third and fourth pairs of values in table 4). In the case of the oxygen-vacancy-centred cluster there is little change in energy between virtual-only and full calculations. For the magnesium-vacancy-centred cluster, the full counterpoise calculation gives rise to a much larger BSSE than does the virtual-only calculation. Which ever method is used, the energy gained by the O_6 cluster is much greater than that gained by the Mg_6 cluster. This is because the O^{2-} ions are much more diffuse than the Mg^{2+} ions and are therefore better able to make use of the additional virtual basis to lower the energy of their diffuse orbitals. This feature is particularly marked for the full counterpoise calculation as there are more basis functions available.

The same effects are observed again in the BSSE calculation on the single (000) ions. The $Mg^{2+}(000)$ ion gains little energy from a virtual O_6 set whereas the $O^{2-}(000)$ ion gains much more energy from the Mg_6 basis. It is also found that for the single O^{2-} ion, a significant change in energy is apparent between the virtual-only and full calculations. Orbital analysis shows that this occurs because in the full calculations the electrons in the diffuse O^{2-} orbitals are being delocalised over the Mg(100) core orbitals centred on an attractive 2+ point-ion site. This situation is unphysical and gives rise to a greatly

Table 5. Basis-set superposition error (BSSE) correction by the virtual-only functional counterpoise method for GAMESS unrelaxed defect formation energies (all energies in eV).

	Uncorrected defect formation energies	Values corrected for BSSE	BSSE energies
V''_{Mg}	36.688	35.167	−1.521
$V^{\cdot\cdot}_{O}$	42.309	40.558	−1.751
Li'_{Mg}	17.670	17.564	−0.106
$Na^{\cdot}_{Mg}$	20.086	20.274	0.188
$Al^{\cdot}_{Mg}$	−23.129	−23.201	−0.072
$F^{\cdot}_{O}$	20.203	18.872	−1.331
$Cl^{\cdot}_{O}$	25.719	26.663	0.944

Table 6. Results for 'unrelaxed' defect formation energies with adjustments to the CASCADE results to account for the effects within the quantum cluster[a]. (All energies in eV).

	Quantum cluster method with unrelaxed nuclear positions	Mott–Littleton unrelaxed	Mott–Littleton allowing (100) oxygen ion shell relaxation
V''_{Mg}	35.167	40.765	30.865
$V^{\cdot\cdot}_{O}$	40.558	40.765	40.765
Li'_{Mg}	17.564	17.540	14.598
$Na^{\cdot}_{Mg}$	20.274	22.964	19.053
$Al^{\cdot}_{Mg}$	−23.201	−23.345	−23.815
$F^{\cdot}_{O}$	18.873	19.117	19.117
$Cl^{\cdot}_{O}$	26.663	25.655	25.655

[a] Basis set is TZV on oxygen, fluorine and chlorine; SV3-21C on magnesium, lithium, sodium and aluminium.

exaggerated BSSE. The isolated Mg^{2+} ion on the other hand has no diffuse electrons that can be delocalised onto the core O^{2-} basis. Values of unrelaxed defect energies corrected for virtual-only basis set superposition errors are presented in table 5.

5. Comparison of methods: cluster size and relaxation effects

5.1. Unrelaxed defect energies

We consider first the results for the unrelaxed defect formation energies starting with the first two columns of table 6. These give results obtained using the two methods entirely without ionic displacement effects. The results show that the values for the oxygen vacancy defect $V^{\cdot\cdot}_{O}$, agree well in both methods, whereas agreement for the magnesium vacancy defect V''_{Mg} is less satisfactory.

The discrepancy arises from the fact that the quantum mechanical approach includes electronic polarisation: even though the nuclear positions in the quantum cluster cal-

culation remain fixed, the electrons in the quantum mechanical cluster polarise in response to the charge of the defect. In the case of V''_{Mg}, the defect centre is surrounded by six oxygen ions (see figure 2) which are polarisable. In the case of $V^{\cdot}_{O}$, the quantum cluster incorporates six magnesium ions, for which polarisation is expected to be very small. Thus, the formation energies for V''_{Mg} using the quantum cluster method should be smaller than with the Mott–Littleton technique as it includes electronic polarisation of the (100) oxygen ions, whereas this component will be absent for $V^{\cdot\cdot}_{O}$.

To confirm this, relaxation of the shell position only was allowed on the (100) oxygen ions in a Mott–Littleton calculation (that is for the magnesium site defects), but the core positions were still held fixed. There is thus electronic polarisation but no ionic displacement. The results of these calculations are shown in the third column of table 6, and comparison of values for V''_{Mg} suggests that the quantum cluster method models approximately 3/5 of the shell-model polarisation energy. Variations from this figure found in the case of the substitutional ion energies, particularly for $Li^{\cdot}_{Mg}$, are thought to be due to problems with the modelling of the lithium–oxygen interaction. However, as will be discussed later, trends in energies between the different substitutional species are modelled well, so that we believe the empiricised potentials are usually quite well matched with the quantum calculations. It is important to remember that with large core–shell displacements, as are being modelled here, the harmonic approximation employed by the Mott–Littleton method will overestimate the (100) oxygen ion shell contribution to the defect formation energy. Conversely, the quantum cluster method will underestimate it due to insufficient flexibility of the basis set and the neglect of correlation terms by the Hartree–Fock method. The basis set flexibility problem can be partially solved by increasing the number of ions in the quantum cluster [16]. The true value will lie somewhere between these values.

5.2. *Relaxation and ionic polarisation*

The next stage in the defect calculations is to consider nuclear relaxations. The simplest relaxation concerns the nearest-neighbour (100) ions of the defect as depicted in figure 2. Unfortunately, if we attempt to relax the quantum mechanically treated ions in a quantum cluster calculation, the ions relax to an unphysical extent as shown in figure 3 for V''_{Mg} because of the lack of a short-range repulsion potential between the ions and the point charges. In order to investigate (100) ion relaxations using quantum cluster method, one must also treat the (200) ions quantum mechanically, and we must use the larger cluster shown in figure 4. This leads to another problem because, as the larger cluster means calculations now involve a larger number of orbitals, so the quality of basis set has to be restricted because of practical computational limits.

In fact, the most complex basis set that can be used in practice on any ion is the SV 3-21G set, previously deemed unsuitable for anions when calculating formation energies. Fortunately this limited basis has been found to give reliable results for relaxation calculations. Calculations involving relatively small displacements of ions already contained in a quantum mechanical cluster seem less dependent on basis set than do calculations involving the addition or removal of complete ions from the cluster. This is illustrated in figure 5 where relaxations of magnesium (100) ions around a $Cl^{\cdot}_{O}$ defect are presented using both TZV and SV 3-21G basis sets on the chloride ion. We can see that the equilibrium relaxations at the minima in the curves, indicated by the two arrows, are very close. In fact the minima differ by only 0.004 Å in displacement and a mere 0.32 eV in relaxation energy. This energy difference is remarkably small when it is considered

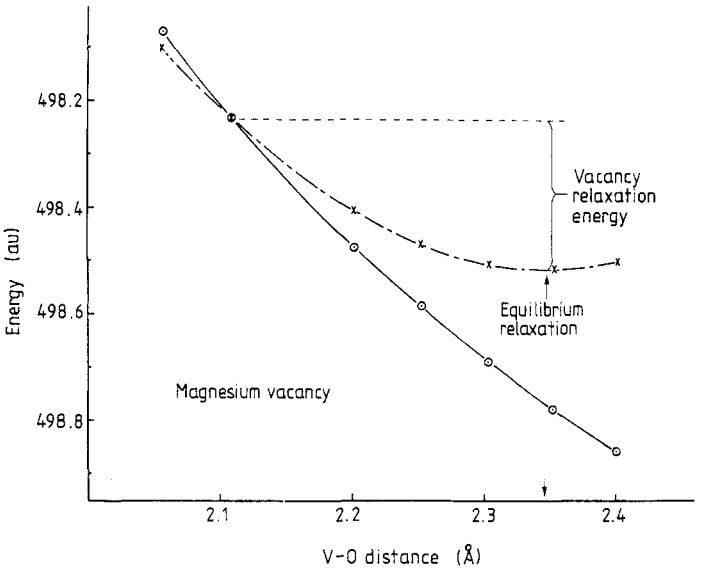

Figure 3. Relaxation of nearest-neighbour (100) ions using the two quantum mechanical cluster sizes. Total energy from GAMESS: ⊙, using small quantum mechanical cluster; ×, using large quantum mechanical cluster.

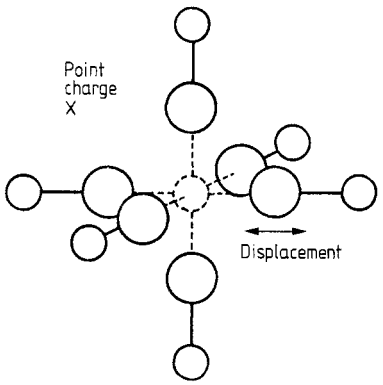

Figure 4. Example of the larger quantum mechanical cluster used to determine the extent of (100) ion relaxation.

that, if the energy scales were not adjusted to make the curves coincide, the curves themselves would be separated by nearly 60 eV.

The reason for the large difference in total energies derives from the better representation of the chlorine core orbitals by the TZV basis; the SV 3-21G basis employs only three Gaussians to describe core orbitals whilst the TZV basis uses six. Although the core orbitals make a large difference to the total cluster energy, they are essentially non-bonding and their superior description by the TZV basis plays no role in deciding the equilibrium geometry. Relaxation calculations using the quantum cluster method therefore employ the SV 3-21G basis set and the large cluster type as in the example shown in figure 4. Using this method, the quantum cluster technique yields physically realistic results, in fair agreement with Mott–Littleton results (see figure 3 and table 7).

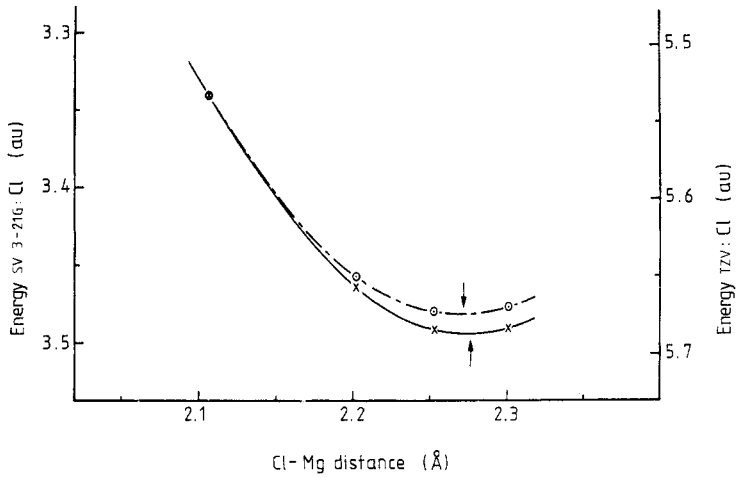

Figure 5. Relaxation of nearest-neighbour (100) ions around a Cl_O defect employing both TZV (⊙) and SV 3-21G (×) basis sets on the chlorine ion within the quantum mechanical cluster of Cl Mg_6O_6.

Once again the Mott–Littleton calculations must be modified slightly so that short-range interactions are computed between the now larger number of ions included in the quantum cluster region I. The results of such calculations are given in table 7. Those labelled CASCADE (A) are calculated excluding the effect of electronic polarisation,

Table 7. Results of nearest-neighbour relaxations: CASCADE (B) results include appropriate shell relaxations; CASCADE (A) do not.

Magnesium site defects				Oxygen site defects			
		Relaxation energy (eV)	(100) ion relaxation distance (10^2 nm)			Relaxaion energy (eV)	(100) ion relaxation distance (10^2 nm)
Mg_{Mg}^{x}	GAMESS	0.027	0.17	O_O^{x}	GAMESS	0.015	0.09
	CASCADE (A)	0.022	−0.04		CASCADE (A)	0.000	0.00
	CASCADE (B)	0.013	−0.04		CASCADE (B)	0.000	0.00
V_{Mg}''	GAMESS	3.041	2.04	$V_O^{\cdot\cdot}$	GAMESS	6.030	2.08
	CASCADE (A)	6.022	2.23		CASCADE (A)	6.053	2.21
	CASCADE (B)	0.913	1.36		CASCADE (B)	6.162	2.23
Li_{Mg}'	GAMESS	0.763	1.09	$F_O^{\cdot}$	GAMESS	1.080	1.02
	CASCADE (A)	0.863	0.88		CASCADE (A)	1.334	1.07
	CASCADE (B)	0.061	0.35		CASCADE (B)	1.348	1.09
Na_{Mg}'	GAMESS	2.075	1.62	$Cl_O^{\cdot}$	GAMESS	4.120	1.51
	CASCADE (A)	2.336	1.36		CASCADE (A)	3.931	1.62
	CASCADE (B)	0.496	0.95		CASCADE (B)	3.971	1.66
$Al_{Mg}^{\cdot}$	GAMESS	1.185	−1.31				
	CASCADE (A)	3.286	−1.66				
	CASCADE (B)	0.946	−1.24				

whilst those marked CASCADE (B) include shell relaxation. Of course, the larger cluster means that polarisation effects are now apparent for defects centred at both lattice sites. However, as the polarisable oxygen ions are much further from the defect site for the oxygen-centred defects, polarisation effects are much smaller for these defects. Hence the difference between CASCADE (A) and (B) values are small for the oxygen-centred $V_O^{\cdot\cdot}$, $F_O^{\cdot}$ and $Cl_O^{\cdot}$, but much larger for the magnesium-centred V''_{Mg}, Li'_{Mg}, Na'_{Mg} and $Al_{Mg}^{\cdot}$.

When calculating Mott–Littleton relaxation energies that include electronic polarisation, it is important to allow electronic polarisation on both the initial unrelaxed geometry and the final relaxed configuration as is the case in the CASCADE (B) results. When modelling the equivalent situation as the larger quantum mechanically treated cluster, this is the difference between the total energies of two clusters. The first cluster represents the starting point and has the (100) nuclear positions fixed but the (100) shells (for magnesium-centred defects) or (200) shells (for oxygen-centred defects) relaxed. The second cluster represents the relaxed geometry and has both the (100) nuclear and the (100) shell or (200) shells relaxed. We should note that for magnesium-centred defects the effect of shell relaxation is greater for the first cluster, where no nuclear relaxation is allowed, than for the second cluster, where both modes of relaxation are allowed and therefore complement each other. It follows that relaxation energies calculated with the inclusion of these polarisation effects (B) are lower than those where this effect is ignored and only nuclear relaxation is considered, that is cases (A). For oxygen-centred defects, shell polarisation is very slightly greater in the relaxed configurations so that CASCADE (A) results are a little lower than CASCADE (B) values (see table 7).

5.3. Trends with species

We can usefully compare trends from species to species as well as the numerical values of energies in assuming the Mott–Littleton and quantum approaches. From table 6 we see that both methods predict that the formation energy of Li'_{Mg} is smaller than for Na'_{Mg}; similarly, that for $F_O^{\cdot}$ is smaller than for $Cl_O^{\cdot}$. Such results would be expected on the basis of ionic radius arguments [17]. It is gratifying that both models exhibit such ionic radius effects so readily.

The same size effect should also be seen in the calculated relaxation energies. Indeed, in table 7 it is seen that the Na'_{Mg} defect causes much larger relaxation of the 100 ions than does Li'_{Mg}, this being a direct result of the lattice accommodating the oversized Na^+ ion. Again, $Cl_O^{\cdot}$ causes greater relaxation than $F_O^{\cdot}$.

5.4. Discrepancies between quantum and classical approaches

Discrepancies between values calculated by the two methods may be due to a number of factors. We consider two points here. First, the central cluster embedded in point charges may not be in equilibrium, and the equilibrium interatomic spacings will normally differ slightly between the classical and quantum cases. Second, the two approaches differ in the way electronic polarisation is handled. We find that neither effect is substantial here. The starting unrelaxed geometry for the quantum mechanical cluster constrains the Mg–O distances to be 2.106 Å, the same as in the bulk oxide. Thus, the perfect lattice geometry for the quantum cluster calculations (that is, Mg_6O_7 for O_O^x and Mg_7O_6 for Mg_{Mg}^x, both in point-charge arrays) will not be precisely in equi-

librium, for there are no short-range forces acting on the quantum cluster from the outer point charges. This effect has been investigated by allowing (100) relaxation of the defect-free quantum clusters, Mg^{x}_{Mg} and O^{x}_{O}. It can be seen from table 7 that the relaxation of these clusters to an equilibrium geometry has a rather small, but not entirely negligible, effect. Relaxation energies might therefore be adjusted accordingly, though we have not carried this out in the present work. The equivalent perfect lattice calculations were carried out using the Mott–Littleton method. It was found that, with the restriction of short-range interaction to region I ions, Mott–Littleton calculations also gave a very small relaxation energy for the magnesium-centred cluster. However, the direction of the relaxation was towards the central ion instead of away from it as in the quantum cluster results.

This points to a more subtle difference between the approaches. The reason is that at these oxygen–oxygen separations, the short-range oxygen–oxygen potential is slightly attractive. This is because this empirical potential is dominated by the $(1/r^6)$ term (see the appendix) which is modelling correlation effects. As mentioned earlier, in the present form, the Hartree–Fock approach does not model correlation effects and so omits any such attractive term. Clearly one might model correlation by carrying out a configuration interaction (CI) calculation on the quantum cluster. This would be extremely costly in computer time and is ignored here as the difference effects are so small. Special attention is needed only in cases for which there is reason to expect the effect might be large.

These aspects are still less important for the oxygen-centred perfect lattice where no relaxation was observed for the CASCADE calculation. This is partly because the Mott–Littleton calculation assumes a zero magnesium–magnesium short-range potential and also because the (100) magnesium–(020) oxygen separations are so large that their non-Coulombic interactions too are also negligible. The quantum cluster calculation also gives a very small relaxation in the equivalent cluster. Overall therefore, the lack of exact equilibrium in the quantum cluster has no significant consequences.

A second possible reason for discrepancies results from the very different ways in which electronic polarisation is treated in the two approaches. In particular we might expect that the quantum cluster calculation would underestimate polarisation because of insufficient flexibility in the basis set. This would be particularly pronounced for the relaxation calculations which use only the less-flexible SV 3-21G basis for the oxygen ions. If so, then the magnesium site defects V''_{Mg}, Li'_{Mg} and Na'_{Mg} (table 7) should give a larger energy from electronic polarisation using the classical Mott–Littleton code than using the quantum GAMESS code. The deficit will be made up from ionic polarisation. Hence the polarisation correction will lead to Mott–Littleton ionic displacement energies (CASCADE (B)) smaller than quantum cluster results (see again table 7). Moreover, since polarisation energies are quadratic in the net charge, this difference will be greater for the higher-charged defect V''_{Mg}. In the same way, if electronic polarisation effects are switched off in the Mott–Littleton calculations, the magnesium-site defects will exhibit relaxation energies (CASCADE (A)) that are greater than those calculated using the quantum cluster technique, as the Mott–Littleton ionic displacements are now responsible for all the relaxation energy, whereas a portion of this energy is taken up in the quantum cluster calculation by electronic polarisation in the unrelaxed configuration. Our results for the V''_{Mg} defect suggest that the SV 3-21G basis will yield about one-half of the electronic polarisation energy that is predicted by Mott–Littleton methodology, whereas the more flexible TZV basis models about three-fifths of this energy.

For the oxygen-site defects, as electronic polarisation takes place only on the (200) ions, and as these polarisable ions are twice as far away from the defect site as their

Table 8. Mott–Littleton results for different relaxation modes on the defect V''_{Mg} and their relationship to the continuum model.

	CASCADE relaxation energy (eV)	Continuum model relaxation energy (eV)
Relaxation of all cores and shells	16.738	12.279
Relaxation of (100) cores and shells	8.375	—
Difference	8.363	8.683
Relaxation of all shells and no cores	11.946	9.116
Relaxation of (100) shells and no cores	6.452	—
Difference	5.494	5.263

equivalents were for the magnesium-site defects, polarisation discrepancies are not nearly so pronounced.

5.5. Longer-range relaxations

The relaxation of the (100) ions alone will certainly not describe the complete relaxation around these defects. However, this nearest-neighbour relaxation mode is often the only one open to direct investigation due to the limited size of usable quantum cluster. How much of the total lattice relaxation energy can this mode be expected to account for? The answer lies in the Mott–Littleton results shown in table 8. Here we compare the relaxation energy for (100) core and shell relaxation with the energy gained if all ions (core and shells) are allowed to relax. The (100) relaxation yields almost exactly one-half of the total relaxation energy.

A similar result is obtained if the effect of shell relaxation only is considered. That is, the nearest-neighbour shell relaxation will account for one-half of the total available shell relaxation (see table 8). By considering the difference between the (100) nearest-neighbour-only relaxation mode and that where all appropriate centres are relaxed, we calculate the relaxation energy associated with ions outside a region or cavity that includes the defect centre and nearest-neighbour ions. This is shown in table 8.

It is of interest in the present context to consider an approximation to relaxation energies associated with cavities of different sizes using a simple dielectric continuum model [18]. In this, the relaxation energy $E(R)$ around a cavity of radius R is given by

$$E(R) = (e^2/2R)(1 - 1/\varepsilon)$$

where e is the effective charge of the defect site and ε is either the optical dielectric constant ε_∞ if we are concerned solely with shell relaxation effects, or it is the static dielectric constant ε_0 if both core and shell relaxation are being modelled. The value of R will be the nearest-neighbour distance a_0 if all ions apart from the defect centre are outside the cavity; it will be $\sqrt{2}a_0$ if both core and shells are relaxed outside a cavity that includes the defect centre and nearest-neighbour ions; and it will be $\sqrt{3}a_0$ if only shells are relaxed outside the nearest-neighbour and central defect cavity. This latter value of R is larger as the second-nearest-neighbour ions are cations and are therefore not considered to be polarisable.

From table 8 we see that this continuum model is modestly successful at describing

Table 9. Potential parameters.

Ion	A	ρ	C
O(2−) . . . O(2−)[a]	22764.3	0.1490	20.37
O(2−) . . . F(1−)[b]	1440.21	0.3027	22.468
O(2−) . . . Cl(1−)[c]	962.95	0.24917	30.054
Mg(2+) . . . F(1−)[b]	2902.29	0.23668	1.866
Mg(2+) . . . Cl(1−)[d]	5171.38	0.2578	0.00
Mg(2+) . . . O(2−)	740.7[e]	0.3478	0.00
	1275.20[f]	0.3012	0.00
Li(1+) . . . O(2−)	292.3[e]	0.3472	0.00
	2515.37[c]	0.2408	25.127
Na(1+) . . . O(2−)	611.1[e]	0.3535	0.00
	1096.88[c]	0.3016	0.00
Al(3+) . . . O(2−)	821.1[e]	0.3449	0.00
	1385.13[c]	0.3009	0.00

[a] Catlow 1974 (reference [22]).
[b] Stoneham 1981 (reference [23]).
[c] Empiricised potential using Lewis electron gas potential (reference [14]) and appropriate empirical potential from Sangster and Stoneham (reference [24]).
[d] Empiricised electron gas potential to the Mg(2+) . . . O(2−).
[e] Lewis electron gas potential (reference [20]).
[f] Potential due to Sangster and Stoneham (reference [24]).

the total relaxation energies ($R = a_0$) for both 'shell-only' and 'shell + core' relaxation types. However, the model gives excellent agreement with those energies calculated by CASCADE for the relaxations beyond the cavity size which includes nearest-neighbour ions.

A large energy value calculated by the Mott–Littleton method when (100) nearest-neighbour ions are included may be expected as there will be a large core–shell displacement involved and this might be overestimated by our harmonic approximation as mentioned in § 5.1.

Table 10. The effect of using empirical and electron gas potentials on defect formation energies (eV).

		Defect formation energy with unrelaxed coordinates (eV)	Defect formation energy after relaxation of cores and shells (eV)
V''_{Mg}	Electron gas	37.184	21.808
	Empirical	40.704	24.295
Li'_{Mg}	Electron gas	17.430	13.782
	Empiricised	17.323	13.650
Na'_{Mg}	Electron gas	23.066	18.112
	Empiricised	22.957	18.002
$Al^{\cdot}_{Mg}$	Electron gas	−23.338	−29.015
	Empiricised	−23.341	−29.163

If it is only practical to relax first neighbours in a cluster calculation, can one use results from the classical approach to improve the predictions? In previous studies [19], relaxed coordinates from CASCADE were employed within the quantum cluster method to try to interface the two methods and to assess the legitimacy of this type of approach. However, there is a problem because of the way long-range Coulombic interactions are included and the limitations of the point-charge cluster: the only lattice sites that experience the correct electrostatic field expected from an infinite lattice simulation are those of the inner region. Therefore, the movement of any outer-region ions would lead to a contribution to the cluster relaxation energy due to the incorrect electrostatic field on these ions. Long-range relaxation energies calculated by the two methods are therefore not strictly comparable. In fact, to model long-range relaxations using quantum clusters, short-range repulsive potentials must be added to the point charges and a continuum correction must be employed to give sound Madelung potentials at ion sites. In short, a consistent interface between the two methods is essential. This approach is being developed at present within the ICECAP code [2, 4].

6. Conclusion

We have made a systematic comparison of classical Mott–Littleton and quantum mechanical Hartree–Fock methods for point defects in oxides. Our results show first that the quantum results do give support to the classical approach and second that this consistency enables us to extend the value and range of properly done calculations on relatively small clusters. In addition, we have studied the size of quantum cluster needed to obtain reliable results and the quality of the basis sets that must be used in such calculations.

Acknowledgment

This work was supported by the General Nuclear Safety Research programme of the UKAEA, which is funded by the Department of Energy.

Appendix. Short-range potential parameters for impurities

The short-range potentials used in the Mott–Littleton calculation are all of a Buckingham form, that is

$$V_{ij}(r) = A_{ij} \exp(-r_{ij}/\rho_{ij}) - C_{ij}/r_{ij}^6$$

where r_{ij} is the internuclear distance between centres i and j. The choice of the potential parameters is obviously of critical importance. Generally, potential parameters are fitted to a variety of structural information, and indeed this has been done to yield reliable Mg–O and O–O potentials for the MgO structure. However, structural information does not exist for the dopant ions; in MgO we must use non-empirical methods (in particular, electron gas methods) to determine a set of consistent potential parameters for all the necessary ion interactions [20].

Previous experience has indicated that poor results will be obtained if potentials from electron gas methods are used indiscriminately with potentials derived from empirical structure fitting [21]. However, although the absolute values of the electron gas poten-

tials may be inconsistent with empirical potentials, the differences between the potentials are expected to be reliable. Hence if, for a reference interaction, the difference in energy ΔV between the electron gas potentials (V^{R}_{EG}) and (V^{*}_{EG}) is determined for a range of interatomic separations, then this is added to values obtained for the reference interaction (V^{R}_{Em}). These new values are then fitted to the original potential form to yield modified (or rather empiricised) electron gas potentials ($V^{*}_{Ep.}$):

$$V^{*}_{Ep}(r_i) = \text{Fitted}\,[(V^{*}_{Em}(r_i) - V^{R}_{EG}(r_i)) + V^{R}_{Em}(r_i)].$$

In this way, we are able to make use of the more reliable empirical short-range potentials whilst maintaining the consistency of electron gas potentials. The values of parameters thus obtained are given in table 9. Table 10 shows the effect that these changes have on calculated defect formation energies. The move from pure electron gas to empiricised potentials increases the V''_{Mg} formation energies by over 3.5 eV, both before and after relaxation. On the other hand, very little change occurs for the three substitutional defects on changing from pure electron gas to empirical and empiricised potentials. Thus, the empiricising process maintains the same consistency between the empirical reference and empiricised potential as was enjoyed by the original electron potentials.

References

[1] Catlow C R A and Mackrodt W C (eds) 1982 *Computer Modelling of Solids, Springer Lecture Notes in Physics* vol 166 (Berlin: Springer) Ch. 1, Ch. 10
[2] Vail J M, Harker A H, Harding J H and Saul P 1984 *J. Phys. C: Solid State Phys.* **17** 3401
[3] Vail J M, Pandey R and Harker A H 1987 *Cryst. Latt. Def. Amorph. Mat.* **15** 13
[4] Harding J H, Harker A H, Keegstra P B, Pandey R, Vail J M and Woodward C 1985 *Physica* B **131** 151
[5] Henderson B 1968 *Adv. Phys.* **17** 749
[6] Hayes W and Stoneham A M 1985 *Defects and Defect Processes in Non-Metallic Solids* (New York: Wiley)
[7] Stoneham A M 1984 *Physics of Binary Oxides* (Seville: University Press) p 85
[8] Norgett M J 1974 *UKAEA Harwell Report R. 7650*
[9] Leslie M 1982 *Program CASCADE, Description of Data sets for Use in Crystal Defect Calculations, SERC Daresbury Laboratory Internal Report DL/SCI/TM31T*
[10] Dick B G and Overhauser A W 1958 *Phys. Rev.* **112** 90
[11] Guest M F, Kendrick J and Poper S A 1983 *GAMESS Documentation, Daresbury Laboratory*
[12] Boys S F and Bernardi F 1970 *Mol. Phys.* **19** 553
[13] Jonsson B and Nelander B 1977 *Chem. Phys.* **25** 263
[14] van Lenthe J H, van Duijnevenldt-van de Rijdt J G C M and van Duijneveldt F B 1987 *Ab initio Methods in Quantum Chemistry II* ed. K P Lawley (New York: Wiley) p 520
[15] Dauley J P, Claverine P and Malrien J P 1974 *Int. J. Quantum Chem.* **8** 1
[16] Grimes R W, Catlow C R A and Stoneham A M 1989 *J. Chem. Soc. Faraday Trans.* **85** 485
[17] Shannon R D 1976 *Acta. Crystallogr.* A **32** 751
[18] Mott N F and Gurney R W 1948 *Electronic Processes in Ionic Crystals* (Oxford: University Press)
[19] Grimes R W, Catlow C R A, Cormack A N and Stoneham A M 1987 *Advances in Ceramics* vol 23 *Non-Stoichiometric Compounds* (Columbus, OH: Am. Ceram. Soc.)
[20] Lewis G V 1984 *PhD Thesis* University of London
[21] Butler V, Catlow C R A, Fender B E F and Harding J H 1983 *Solid State Ionics* **8** 109
[22] Catlow C R A 1977 *Proc. R. Soc.* A **353** 533
[23] Stoneham A M 1981 *Handbook of Interatomic Potentials. I. Ionic Crystals* (*AERE-R. 9598*) (Harwell, UK: AERE)
[24] Sangster M J L and Stoneham A M 1981 *Phil. Mag.* B **43** 597